I N T E R N A L W A V E S

in the Gulf of California

A Thesis
by
Walter H. Munk

In Partial Fulfilment of the Requirements
for the Degree of Master of Science

California Institute of Technology
Pasadena, California
1940

The writer wishes to acknowledge the help of Dr. H.U.Sverdrup, Director of the Scripps Institution of Oceanography, without whose advise and encouragement this investigation could not have been completed. He was the first to suspect the occurence of an internal wave in the Gulf of California. Dr. Sverdrup carried out a preliminary investigation, and the first part of this thesis, dealing with observations, is due to him.

We are also indebted to Dr. H.Bateman, Professor of Mathematics at the California Institute of Technology for his help in finding a solution to the general differential equation, and to Mr. F.Brunner for having carried out many of the tedious calculations.

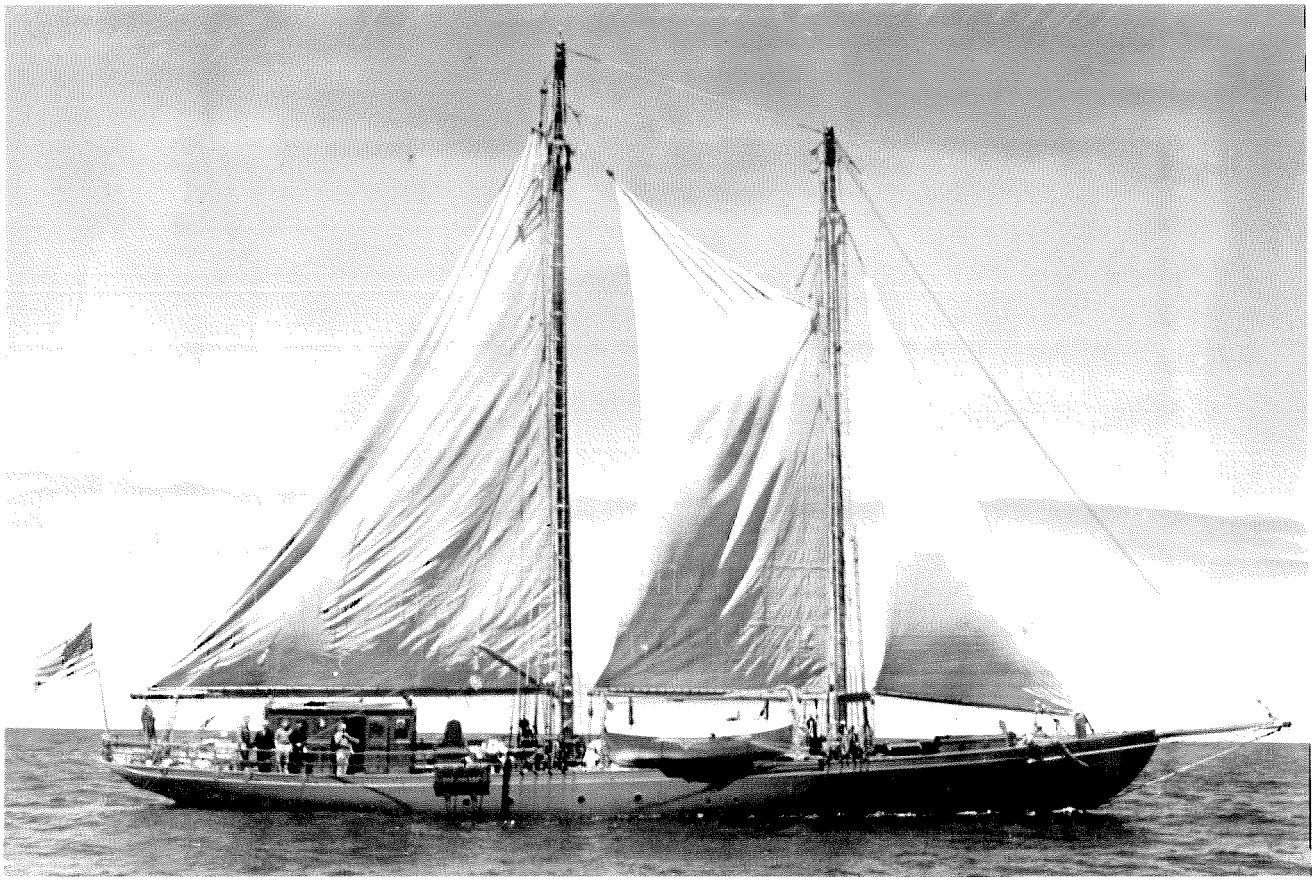

The "E.W.Scripps"

from which measurements

which lead to this investigation were taken.

INTRODUCTION

Between February 13 and March 19 1939 the "E.W.Scripps", research vessel of the Scripps Institution of Oceanography, occupied 53 oceanographic stations in the Gulf of California. The observations of temperature, salinity and oxygen content, which at every station were taken at a series of depths, suggested the existance of internal waves with amplitudes as large as one tenth the depth of the Gulf.

Waves generally can be classified into short and long waves and both groups comprise surface and internal waves, with frequencies corresponding to free or forced oscillations, and of the standing or progressive wave types. Those under consideration are of the "long, internal, free, standing wave" type, perhaps the least known of the sixteen possible combinations. It is the object of this paper to present a discussion of these waves from both an observational and theoretical point of view and to compare the results.

The bottom topography of the Gulf is quite complicated but the average depth remains nearly constant to a considerable distance from the entrance and decreases

then regularly. We know qualitatively that velocity of propagation decreases with decreasing depth. With this in mind we first find that all observations can be combined to a consistent picture from which we obtain the period of oscillation and the wavelengths.

A theoretical treatment of the outer portion of the Gulf, applying FJELDSTAD's theory for internal waves at constant depth (1) yields results in good agreement with those indicated by observation. For the inner portion of the Gulf a general theory for internal waves in a basin of non-constant depth is developed and applied. FJELDSTAD's theory is also expanded to include the case of a horizontal density gradient.

The results of the theory, applied to the Gulf of California, compare favorably to those obtained by the observational approach.

RESULTS FROM DIRECT OBSERVATION

The Gulf of California is the southern end of the group of the great Pacific depressions, which extend roughly paralell to the coast perhaps as far north as Alaska. The Gulf follows a straight course throughout its length of 1100 km. This linearity is a consequence of its tectonic origin, for the Gulf of California is most likely associated with the large San Andreas fault system. Its exceptional symmetry makes it remarkably suited for the existance of large periodic movements of its water mass.

A study of the currents in the outer portions of the Gulf led at first to very discouraging results. The dynamical topography of the surface relative to the 1500 decibar surface does not indicate

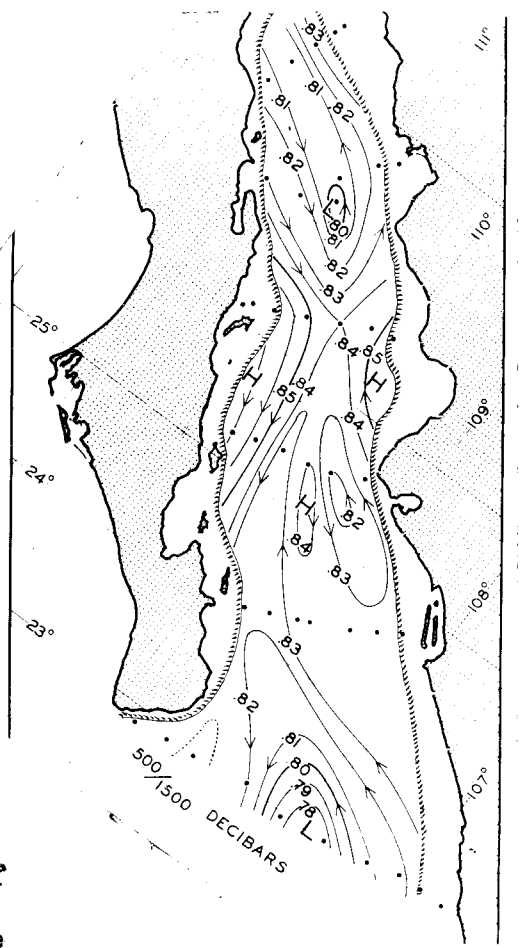

Fig.1

any regular exchange of water between the Gulf and the adjacent part of the Pacific but shows a sequence of seperate highs and lows. (Fig.1) The highs and lows are associated with alternating downward and upward displacements of the isopycnic surfaces.

Let $\rho_{o,t,s}$ be the density, depending upon the oxygen content, temperature and salinity of the water. The vertical displacements, as represented by

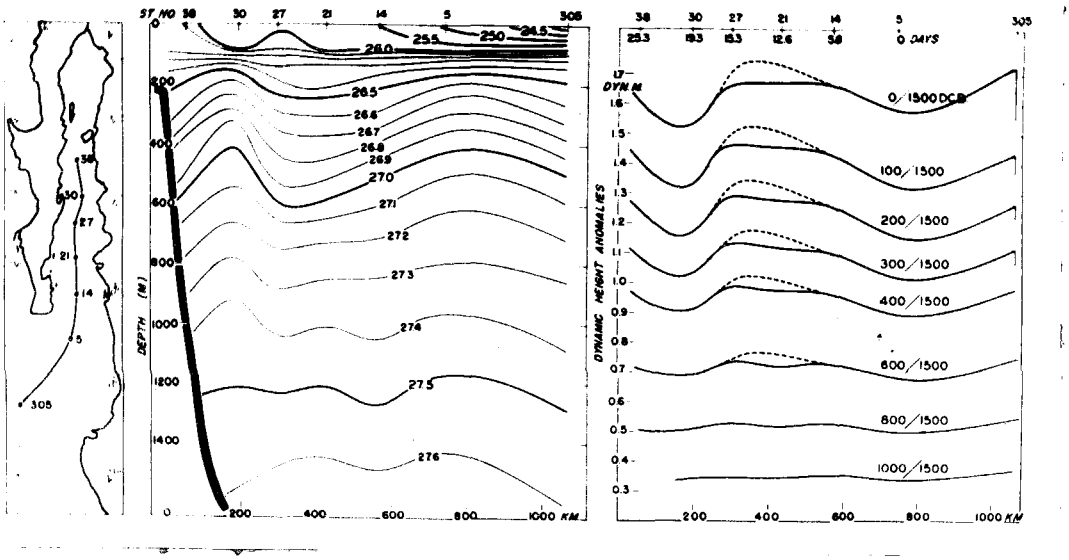

Fig.2

σ_t-curves ($\sigma_t = 10^3(\rho_{...}-1)$, are clearly seen in a longitudinal section, (Fig.2) based on data from stations along the center line of the Gulf. All stations used for the construction of this section are indicated on the small map on the left of the figure. It should be observed that the vertical scale is highly exaggerated

relative to the horizontal, the ratio between vertical and horizontal scales being equal to 1/800. The profiles of a series of isobaric surfaces relative to the 1500 decibar surface are shown to the right of the figure.

The wavy character of the curves suggests the possibility that they may be associated with a standing internal wave. The observations are not simultaneous, but at the top right hand corner of the figure is shown the number of days elapsed between occupation of station 5, the central station at the southern section, and the other stations used for constructing the profile. It is evident that if the observations indicate a standing wave, the wave period must be such that when travelling up the Gulf the vessel remained nearly in phase with the wave. This gives immediately an indication of the possible period length. Station 14 appears to have been occupied near a nodeof the wave, and in this case the time difference is of no importance. Station 21 appears to have been occupied shortly before the wave reached its highest value, and the wave period must therefore have been greater than 12.6/2, that means greater than 6.3 days. Station 27 was occupied after the wave reached its crest and the wave period must

therefore have been less than 15.3/2, which means less than 7.65 days. Station 30 appears to have reached approximately at the time when the wave at the surface reached its lowest position and the wave period must therefore be approximately 19.3/3, which means approximately 6.4 days. Finally, Station 38 must have been reached nearly at the time of greatest elevation. Therefore the period must be approximately 25.3/4, that means 6.3 days.

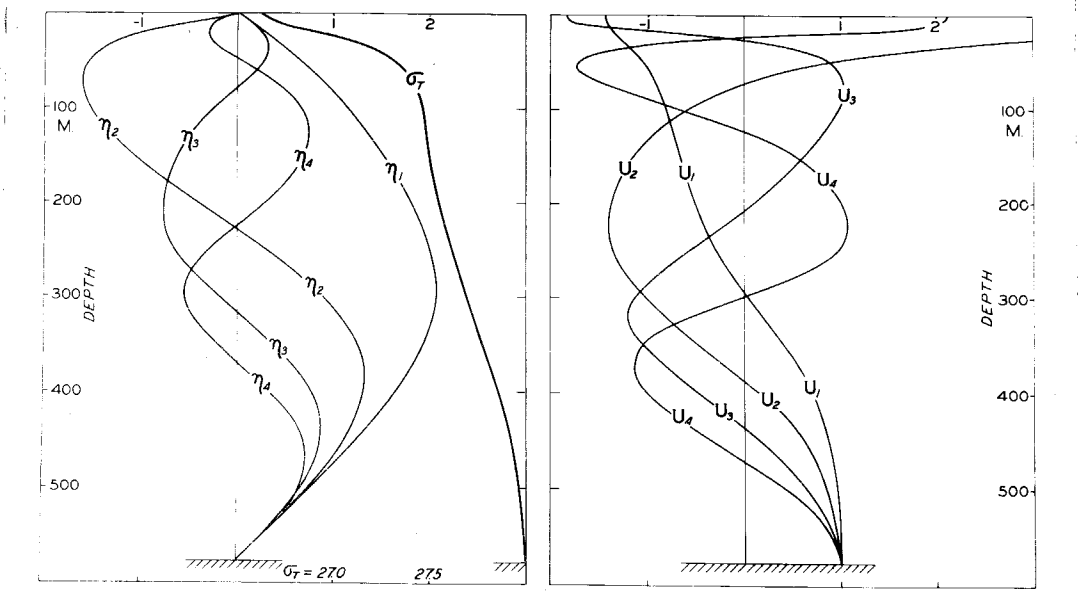

Fig.3

This merely indicates that if the wavy character of the isobaric surface is due to an internal wave, its period would lie between 6.3 and 7.65 days, and probably closer to the former value. Before we can decide in favor

of this explanation we must make sure that it does not conflict with any other laws governing internal waves. A general discussion of these laws has been presented by SVERDRUP (4) and DEFANT (2).

The internal wave is considered here in two dimensions: A vertical axis and a horizontal axis along the center line of the Gulf. Harmonics may develop with respect to both the horizontal and the vertical coordinate. Fig.3 illustrates waves of the first, second and third order with respect to the vertical axis. On the left side we have plotted maximum vertical displacement against depth, or, since they are proportional, maximum vertical velocity against depth. This velocity component vanishes at top and bottom, and shows maxima, equal in number to the order of the waves. To the right the horizontal velocity component has been plotted against depth. It is evident from the σ_t curves that one has mainly to deal with an internal wave of the first order. The maximum amplitude lies between 500 and 600 meters and is of the order of magnitude of nearly 100 meters.

Amplitudes of the internal wave become small near the surface and the bottom of the ocean. LAMB (3) calculated the ratio of the amplitude at the free surface

to the maximum amplitude:

$$\frac{A_s}{A_m} = \left(\frac{\rho_1}{\rho} - 1\right) e^{-kh} \approx 8.2 \times 10^{-4}$$

where h refers to the depth of the maximum amplitude, ρ is the average density above this depth, ρ_1 the average density beneath this depth. $k = 2/\text{wave-length}$.

Our value for A_m = 100 meters indicates an amplitude of only 8 cm at the surface. This is in accordance with the σ_t curves and also with tidal records taken at Mazatlan during this period. These records are not sufficiently accurate to measure such small oscillations but they show that after elimination of the regular diurnal and semi-diurnal components a long period oscillation of amplitude larger than 10 cm did not exist.

The amplitude at the bottom would be zero if the Gulf were of constant depth. Figure 4 will serve to illustrate the topography of the region. It represents a longitudinal section of the Gulf, with six profile planes, intersecting the center line M-N at points A to F, turned clockwise into the plane of the graph. These profile planes are drawn to scale but it should be noted that the vertical scale is highly exaggerated. at the top of the figure we have indicated the actual position

of the stations, from which these profile planes were measured. The bottom of the Gulf appears so irregular that it is difficult to construct what may be called the "effective" depth. From observations at the deepest stations it appears that continous communication between the various depressions is present only above 2000 meters. It seemed

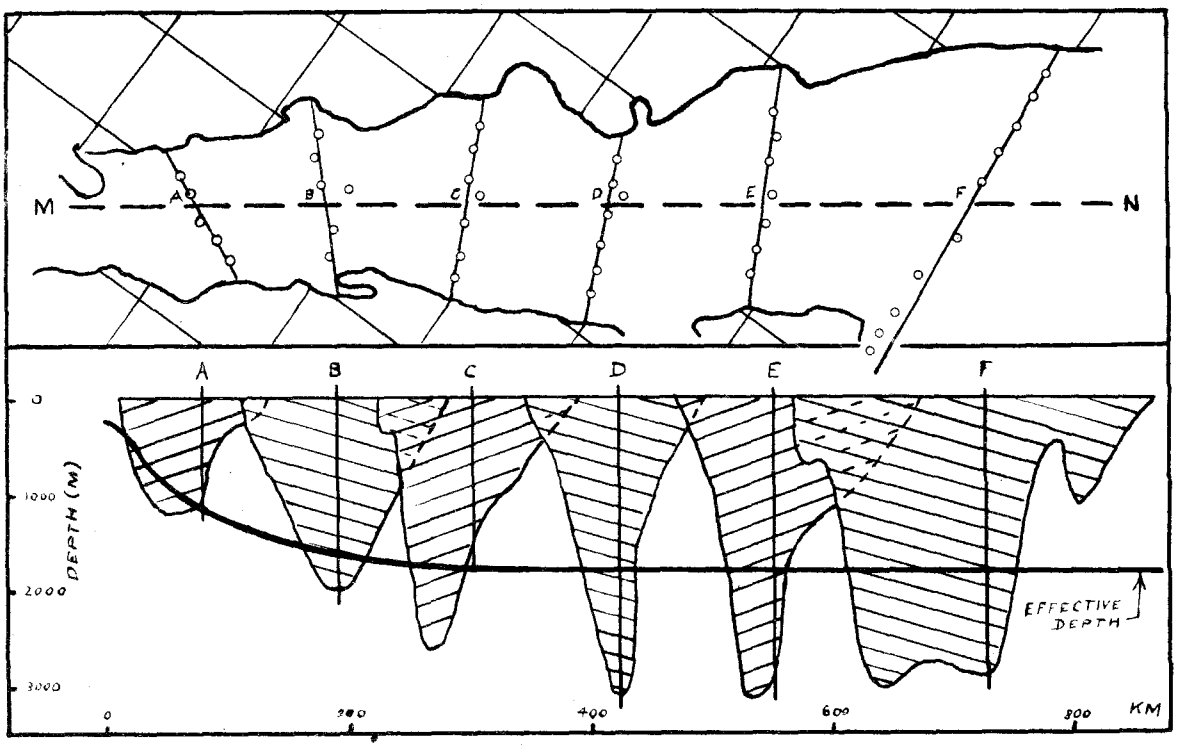

Fig.4

advisable to choose an "effective" depth which remains close to 1800 meters throughout the larger portion of the Gulf. The vertical displacements at the bottom must be negligible

in this region, and this is substantiated by the σ_t curves.

Furthermore there must be a node at the entrance of the Gulf, an anti-node at the inside end, if we are dealing with a free standing wave. At about 29° latitude the channel becomes very shallow, and two islands, San Esteban and San Lorenzo rise above the

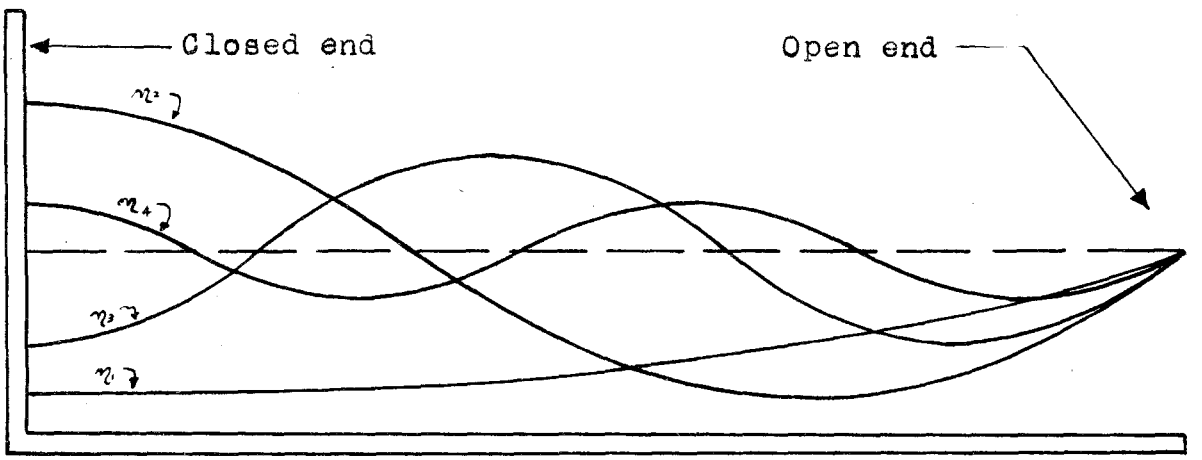

Fig.5

surface. Waves will be reflected before they reach this point or loose their energy by friction and interference. Hence we may consider this the inner end of the Gulf, and may neglect the portion north of the islands, although the Gulf deepens and widens again, and extends 350 km further inland.

The σ_t curves clearly show the existance of an antinode at this location. However, a node is formed not at the actual mouth of the Gulf but about 150 miles further south, near station #305. (Figures 1 and 2). It is generally known that the "effective" length of a canal with regard to a wave phenomenom is not identical with its actual length, but depends upon its width at the open end. A correction formula has been derived for this "Mündungskorrektion":

$$l_e = l_a \sqrt{1 + \frac{2b}{\pi l_a}\left(0.9228 - \ln\frac{\pi b}{4 l_a}\right)} \approx 1.2\, l_a$$

where l_e is the effective length, l_a the actual length, b the width at the mouth. Hence the Mündungskorrektion "lnegthens" the Gulf rougly by 20% and gives an effective length of 1000 km. This is only a first approximation, but it shows good agreement with the σ_t curves.

Between the outer and inner boundary of the Gulf, three nodes can be located. (Fig.2) Figure 5 illustrates standing waves of the first, second, third and fourth order in an half-open channel. We have plotted maximum vertical displacement (or, since they are proportional, the maximum vertical velocity component) throughout its length. A comparison of figures 2 and 5 shows that we are dealing with a wave of the

fourth order with regard to the horizontal coordinate.

Finally the velocity of propagation and hence the wave length decreases when the depth to the bottom decreases. The σ_t curves clearly show a decrease of wave length towards the inner end of the Gulf.

Hence a free, internal, standing wave of first order with respect to the vertical axis and of fourth order with respect to the horizontal axis is in good agreement with the dynamical topography of the Gulf, and obeys all boundary conditions. Observations indicate a period of 6.6 days. A wave length of 1000 km near the mouth of the Gulf gives a velocity of propagation of 175 cm/second, decreasing towards the inside. It is the aim of the following investigation to examine if this picture , which has been derived from observation, is in agreement with theoretical considerations.

THEORETICAL INVESTIGATION

Internal Waves at Variable Depth

The velocity of propagation of a wave depends generally upon the depth to the bottom and the density distribution of the water in which it takes place. FJELDSTAD (1) has treated the case of constant depth and a density distribution which does not change in in a horizontal direction. We shall first treat the case applying to the Gulf of California, that of variable depth but of a negligible horizontal density gradient. Later we shall deal with a basin of constant depth but an appreciable density gradient. The general case, that of variable depth and density appears very complicated and is not treated here.

Previous investigations of wave phenomena (DEFANT, 2) have shown that in a long narrow channel the earth's rotation will tend to produce oscillations in a plane perpendicular to the length of the channel, but its effect upon the chief wave motion along the channel will be small and can in first approximation be neglected. For that reason the problem reduces to a two-dimensional analysis.

We shall assume the x-axis along the direction of propagation of the wave, the z-axis perpendicular to

the surface, where z = 0 represents the undisturbed surface, z = h the bottom. (Fig. 6) Let u and w represent the components of the velocity of the water along the x and z axes respectively, ρ the density, p the pressure, the vertical displacement of a definite particle of water from its position of equilibrium, and g the gravitational constant.

We shall at first proceed in a manner similar to that of FJELDSTAD.

The equations of motion are:

$$\frac{du}{dt} + \frac{1}{\rho}\frac{\partial p}{\partial x} = 0 \qquad 1a$$

$$\frac{dw}{dt} + \frac{1}{\rho}\frac{\partial p}{\partial z} + g = 0 \qquad 1b$$

Assuming the water as incompressible the equation of continuity becomes

$$\frac{\partial u}{\partial x} + \frac{\partial w}{\partial z} = 0 \qquad 1c$$

The density of a particle remains unchanged with time.

$$\frac{d\rho}{dt} = 0 \quad \text{or}$$

$$\frac{\partial \rho}{\partial t} + u\frac{\partial \rho}{\partial x} + w\frac{\partial \rho}{\partial z} = 0 \qquad 1d$$

Numerical values warrant the following adjustments. Let $\rho_{o(z)}$ denote the density in equilibrium condition. We define ρ_1 by

$$\rho = \rho_{o(z)} + \rho_{1(x,z,t)} \qquad 2a$$

Let p_a denote the atmospheric pressure, and $p_{o(z)}$ the pressure due to water in the equilibrium condition.

$$p_{o(z)} = g\int_{o}^{z} \rho_{o(z)}\, dz \qquad 2b$$

and define p_1 by

$$p = p_a + p_o(z) + p_1(xzt) \qquad 2c$$

We obtain by differentiation

$$\frac{\partial \rho}{\partial t} = \frac{\partial \rho_1}{\partial t} \qquad 3a$$

$$\frac{1}{\rho}\frac{\partial p}{\partial x} \approx \frac{1}{\rho_o}\frac{\partial p_1}{\partial x} \qquad 3b$$

$$\frac{1}{\rho}\frac{\partial p}{\partial z} = -\frac{g\rho_o}{\rho_o+\rho_1} + \frac{1}{\rho_o}\frac{\partial p_1}{\partial z}$$

$$g + \frac{1}{\rho}\frac{\partial p}{\partial z} = \frac{g\rho_1}{\rho_o} + \frac{1}{\rho_o}\frac{\partial p_1}{\partial z} \qquad 3c$$

We may assume

$$\frac{du}{dt} = \frac{\partial u}{\partial t},\quad \frac{dw}{dt} = \frac{\partial w}{\partial t},\quad \frac{\partial \rho}{\partial z} = \frac{\partial \rho_o}{\partial z},\quad u\frac{\partial \rho}{\partial x} \ll w\frac{\partial \rho}{\partial z} \qquad 3d$$

Substituting equations 3 into equations 1 we obtain

$$\frac{\partial u}{\partial t} + \frac{1}{\rho_o}\frac{\partial p_1}{\partial x} = 0 \qquad 4a$$

$$\frac{\partial w}{\partial t} + g\frac{\rho_1}{\rho_o} + \frac{1}{\rho_o}\frac{\partial p_1}{\partial z} = 0 \qquad 4b$$

$$\frac{\partial u}{\partial x} + \frac{\partial w}{\partial z} = 0 \qquad 4c$$

$$\frac{\partial \rho_1}{\partial t} + w\frac{\partial \rho_o}{\partial z} = 0 \qquad 4d$$

We shall investigate a standing wave with period $T = \frac{2\pi}{\sigma}$ and wave length $l = \frac{2\pi}{k}$ and velocity of

propagation $c = \frac{\sigma}{k}$. Equations 4 are general since they deal with the properties of an incompressible medium and are quite independent of boundary conditions. FJELDSTAD assumes solutions of the type

$$w(xzt) = W(z)\sin(kx)\cos(\sigma t) \qquad 5a$$

$$u(xzt) = U(z)\cos(kx)\cos(\sigma t) \qquad 5b$$

$$p(xzt) = P(z)\sin(kx)\sin(\sigma t) \qquad 5c$$

$$\rho(xzt) = R(z)\sin(kx)\sin(\sigma t) \qquad 5d$$

With these assumed solutions substituted into equations 4, we have four equations in four unknowns. Solving for $W_{(z)}$ we obtain

$$\frac{d^2W}{dz^2} + \lambda^2 g \gamma W = 0 \qquad \text{where } \gamma = -\frac{1}{\rho_0}\frac{\partial \rho_0}{\partial z},\ \lambda = \frac{1}{c} \qquad 6a$$

subject to the boundary conditions

$$W = 0 \text{ for } z = 0 \text{ and } W = 0 \text{ for } z = h \qquad 6b$$

for the case of constant depth. $W = f(z)$ only, and the subscripts have been omitted in equations 6. A numerical integration between these boundaries (page 50) determines various values of the parameter and hence the velocity of propagation. We shall now show that assumptions 5 leading to equation 6a are inconsistent with the general problem, and furthermore are consistent only if the slope of the bottom is equal to zero.

Consider a channel of uniform width, but variable depth. (Fig. 6) The total amount of water transported through a section K-L per unit time is equal to U dz.

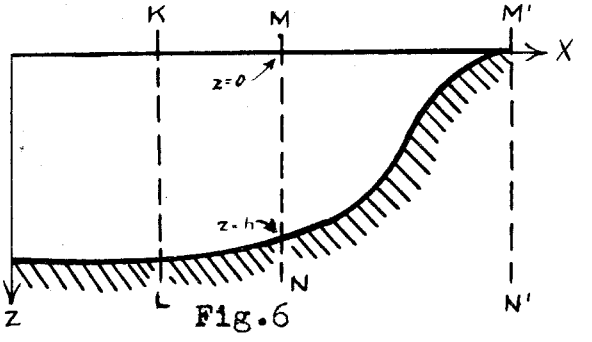

Fig.6

Take any other cross-section M-N. Since the surface of the water between the two cross-sections remains at constant level the transport through M-N must be equal to the transport through K-L. Hence generally

$$\frac{\partial}{\partial x}\int_0^h U_{(xz)}\,dz = 0 \qquad 7$$

We shall now establish the same result by mathematical analogy. Assume that u and w are in phase with regard to time, so that

$$u(xzt) = U(xz).f(t)$$

$$w(xzt) = W(xz).f(t)$$

This is in agreement with our understanding of standing waves generally. Substitute into equation of continuity (1c) and integrate:

$$\int_0^h \frac{\partial U_{(xz)}}{\partial x}\,dz = -\int_0^h \frac{\partial W_{(xz)}}{\partial z}\,dz \qquad 8a$$

We note that generally

$$\frac{\partial}{\partial x}\int_o^h U_{(xz)}\,dz = \frac{\partial h}{\partial x}U_{(xh)} + \int_o^h \frac{\partial U_{(xz)}}{\partial x}\,dz \qquad 8b$$

and hence, noting that the slope of the bottom $m = \frac{\partial h}{\partial x}$

$$-m\,U_{(xh)} + \frac{\partial}{\partial x}\int_o^h U_{(xz)}\,dz = -\int_o^h \frac{\partial W_{(xz)}}{\partial z}\,dz$$

$$= -\left(W_{(xh)} - W_{(xo)}\right) \qquad 8c$$

From 6a we note that $W_{(xo)} = 0$

The kinematic boundary condition at the bottom, namely that all flow must take place along the boundary, is expressed by

$$W_{(xh)} = m(x).U_{(xh)} \qquad 8d$$

and equation 7 follows from 8c.

Change position of M-N until it occupies position of M'-N'. Here the total transport is zero. in view of equation 7 we finally obtain

$$\int_o^h U_{(xz)}\,dz = 0 \qquad 9$$

Let us assume a solution of type 5, or let

$$U_{(xz)} = f(x).f(z)$$

Substituting into equation 7 we obtain

$$\frac{\partial}{\partial x}\int_o^h f(x)\,f(z)\,dz = 0$$

$$\left(\frac{\partial f(x)}{\partial x}\right)\left(\int_o^h f(z)\,dz\right) + \left(f(x)\right)\left(\frac{\partial}{\partial x}\int_o^h f(z)\,dz\right) = 0$$

$$\left(\frac{\partial f(x)}{\partial x}\right)\left(\int_o^h f(z)\,dz\right) + \left(f(x)\right)\left(\frac{\partial h}{\partial x}\,f(h)\right) = 0$$

From equation 9

$$\int_0^h f(x)\, f(z)\, dz = 0, \qquad \text{and hence} \quad \int_0^h f(z)\, dz = 0$$

Together $f(x).f(h)\frac{\partial h}{\partial x} = 0$

$$U_{(xh)}.m = 0$$

$$W_{(xh)} = 0 \qquad 10a$$

According to the kinematic boundary condition 8d

$$W_{(xh)} = m.U_{(xh)}$$

For that reason assumed solutions 5 are inconsistent except for the case in which m = 0.

Proceeding in similar manner it can be shown that a solution of the type

$$U_{(xz)} = \sum_{i=1}^{n} f_i(x).f_i(z)$$

is consistent for values of n larger than one. For the case n = 2, equation 7 leads to

$$\left(\frac{\partial f_1(x)}{\partial x}\right)\left(\int_0^h f_1(z)\, dz\right) + \left(\frac{\partial f_2(x)}{\partial x}\right)\left(\int_0^h f_2(z)\, dz\right) + m\left(f_1(x)\, f_1(z) + f_2(x)\, f_2(z)\right) = 0$$

equation 9 leads to

$$f_1(x)\int_0^h f_1(z)\, dz + f_2(x)\int_0^h f_2(z)\, dz = 0$$

Here the assumed solutions are consistent with the kinematic boundary condition without "m" having to vanish.

Hence we have shown that solutions 5, although applicable to the case of constant depth, cannot be used for the general case of variable depth. We shall now assume a more general solution:

$$u(xzt) = U(xz).\cos(\sigma t) \qquad 11a$$

$$w(xzt) = W(xz).\cos(\sigma t) \qquad 11b$$

$$p_1(xzt) = P_1(xz).\sin(\sigma t) \qquad 11c$$

$$\rho_1(xzt) = R_1(xz).\sin(\sigma t) \qquad 11d$$

Substituting these into equations 4 we can eliminate all functions of time:

$$-\sigma U + \frac{1}{\rho_0}\frac{\partial P_1}{\partial x} = 0 \qquad 12a$$

$$-\sigma W + g\frac{R_1}{\rho_0} + \frac{1}{\rho_0}\frac{\partial P_1}{\partial z} = 0 \qquad 12b$$

$$\frac{\partial U}{\partial x} + \frac{\partial W}{\partial z} = 0 \qquad 12c$$

$$\sigma R_1 + W\frac{\partial \rho_0}{\partial z} = 0 \qquad 12d$$

Differentiating 12a $\quad -\sigma\frac{\partial U}{\partial x} + \frac{1}{\rho_0}\frac{\partial^2 P_1}{\partial x^2} = 0$

Substituting from 12c $\quad \sigma\frac{\partial W}{\partial z} + \frac{1}{\rho_0}\frac{\partial^2 P_1}{\partial x^2} = 0$

and differentiating again

$$\frac{\partial^3 P_1}{\partial x^2 \partial z} = -\sigma\rho_0\frac{\partial^2 W}{\partial z^2} - \sigma\frac{\partial W}{\partial z}\frac{\partial \rho_0}{\partial z} \qquad 13a$$

Differentiating 12b

$$-\sigma\frac{\partial^2 W}{\partial x^2} + \frac{g}{\rho_0}\frac{\partial^2 R_1}{\partial x^2} + \frac{1}{\rho_0}\frac{\partial^3 P_1}{\partial x^2 \partial z} = 0 \qquad 13b$$

Differentiating 12d

$$\frac{\partial^2 R_i}{\partial x^2} = \frac{1}{\sigma}\frac{\partial^2 W}{\partial x^2}\frac{\partial \rho_o}{\partial z} \qquad 13c$$

Substitute 13a and 13c into 13b, and rearrange

$$\frac{\partial^2 W}{\partial x^2}(g\varphi - \sigma^2) - \sigma^2\left(\frac{\partial^2 W}{\partial z^2} - \varphi\frac{\partial W}{\partial z}\right) = 0 \qquad 14a$$

where $$\varphi = -\frac{1}{\rho_o}\frac{\partial \rho_o}{\partial z} \qquad 14b$$

But we find $g\varphi \gg \sigma^2$, $\frac{\partial^2 W}{\partial z^2} \gg \varphi\frac{\partial W}{\partial z}$ 14c

and obtain finally

$$\frac{\partial^2 W_{(xz)}}{\partial z^2} - \frac{g\varphi_{(z)}}{\sigma^2}\frac{\partial^2 W_{(xz)}}{\partial x^2} = 0 \qquad 15$$

For the substitution $W_{(xz)} = W_{(z)}.\sin(kx)$ equation 15 reduces to FJELDSTAD's equation 6a.

Only equations referring to standing waves have been used in this derivation. Consider the standing wave as a superposition of two progressive waves of equal amplitude and speed but opposite direction.

PROGRESSIVE		RETROGRESSIVE	
$u_p(xzt) = U'(xz)\sin(kx-\sigma t)$		$u_r(xzt) = U'(xz)\sin(kx-\sigma t)$	16a
$w_p(xzt) = W'(xz)\cos(kx-\sigma t)$		$w_r(xzt) = W'(xz)\cos(kx-\sigma t)$	16b
$P_p(xzt) = P_i'(xz)\sin(-kx-\sigma t)$		$P_r(xzt) = P_i'(xz)\sin(kx-\sigma t)$	16c
$\rho_p(xzt) = R_i'(xz)\sin(-kx-\sigma t)$		$\rho_r(xzt) = R_i'(xz)\sin(kx-\sigma t)$	16d

Let $2U'(xz)\sin(kx) = U(xz)$

$2W'(xz)\cos(kx) = W(xz)$

$2P_i'(xz)\cos(kx) = P_i(xz)$

$2R_i'(xz)\cos(kx) = R_i(xz)$

Then $u_p - u_r = u_s$

$w_p - w_r = w_s$ ... etc, where u_s and w_s refer to equations 11. Hence the solutions for standing waves are the sum of two particular solutions, referring to progressive waves.

It can be shown that either particular solution 16 satisfies the four basic laws of hydrodynamics and leads to the differential equation 15. Nevertheless solutions 16 cannot be applied to a basin of variable depth. For the ratio w/u at all points along the bottom must equal the slope at these positions, and therefore remain constant with time. In case of standing waves the velocity components are in phase and

$$\frac{w(xzt)}{u(xzt)} = \frac{W(xz)\cos(\sigma t)}{U(xz)\cos(\sigma t)} = \left(\frac{W}{U}\right)_{(xz)}$$

depending upon position only. The velocity component of a progressive wave are out of phase

$$\frac{w_p(xzt)}{u_p(xzt)} = \frac{W'(xz)\cos(kx-\sigma t)}{U'(xz)\sin(kx-\sigma t)} = \left(\frac{W'}{U'}\right)_{(xz)} \cot(kx-\sigma t)$$

and a function of time.Only for m = 0 , since w becomes zero at bottom, the ratio w/u will always be zero and independent of time.

Otherwise equations 16, although satisfying

the equations of hydrodynamics, do not satisfy the conditions demanded by a sloping boundary. A standing wave can exist in a basin where it is impossible for either of the two progressive waves, which may be considered as making up the standing wave, to exist.

We have based this investigation upon the fundamental equations of hydrodynamics. These four equations relate four properties, vertical and horizontal velocity components, density and pressure. Solving for the vertical velocity component we obtain a differential equation with a parameter proportional to the square of the period of vibration. Distinct values of this parameter (Eigenwerte) can be obtained from boundary conditions.

In FJELDSTAD's simpler case this parameter is inversely proportional to the square of the velocity of propagation, and can be evaluated from the top and bottom boundaries. The periods of vibration can easily be computed, once the velocity of propagation and the length of the basin are known. In the general case one single operation involving all four boundaries will yield directly the period of vibration.

Methods of numerical solution.

It now becomes our task to evaluate σ from the differential equation

$$\frac{\partial^2 W_{(xz)}}{\partial z^2} \quad \frac{g\,\varphi_{(z)}}{\sigma^2} \quad \frac{\partial^2 W_{(xz)}}{\partial x^2} = 0 \qquad 15$$

subject to the boundary conditions

$W_{(oz)} = 0$ along $x = 0$ 18a

$W_{(xo)} = 0$ along $z = 0$ 18b

$W_{(xz)} = m_{(x)} \cdot U_{(xz)}$ along the bottom. 18d

This becomes complicated, because φ varies usually very irregularly with depth (Fig. 12). Solutions to the differential equation 15 for $\varphi = a - \frac{b}{z}$ and $\varphi = a - \frac{b}{z} - \frac{c}{z^2}$ are discussed by Th. Sexl. (5 and 6). If this approximation can be applied, and depth expressed as simple function of x, an algebraic method may be called for.

It will usually be necessary to employ a method of numerical integration. The following method is of use if the period of oscillation and the velocity distribution are known from actual measurements and only to be substantiated by theory. Divide a longitudinal cross-section into a great many squares and insert values of W as suggested by observation and boundary conditions.

Calculate the value of the parameter corresponding to the observed period. Equation 15 is transformed into the difference equation:

$$\frac{W_U - 2W_0 + W_D}{(\Delta z)^2} - \frac{g\varphi}{\sigma^2}\,\frac{W_L - 2W_0 + W_R}{(\Delta x)^2} = 0 \qquad 19a$$

$$W_0 = \frac{W_U + W_D - \frac{g\varphi}{\sigma^2}\left(\frac{\Delta z}{\Delta x}\right)^2 (W_L + W_R)}{2\left(1 - \frac{g\varphi}{\sigma^2}\left(\frac{\Delta z}{\Delta x}\right)^2\right)} \qquad 19b$$

where the various letters indicate the assumed values of W in the surrounding squares (Fig.7).

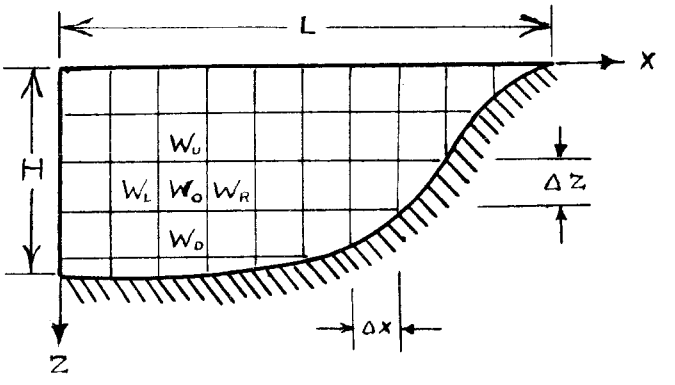

Fig.7

In this manner equation 15 is applied locally, and by covering the entire cross-section we obtain corrected values for W satisfying more closely the differential equation. If we have chosen a proper period and repeat this process a sufficient number of times, the relationship will become smooth and corrections will decrease.

Along the x and z axis proper boundary values were introduced initially and remained unchanged. Along the bottom the kinematic boundary condition must be fulfilled, or

$$W = mU.$$

We can eliminate U by solving simultaenously with the equation of continuity 1c

$$\frac{\partial U}{\partial x} + \frac{\partial W}{\partial z} = 0 \qquad \text{, and obtain}$$

$$\frac{\partial}{\partial x}\left(\frac{W}{m}\right) + \frac{\partial W}{\partial z} = 0 \qquad \text{or}$$

$$m^2 \frac{\partial W}{\partial z} + m \frac{\partial W}{\partial x} - W \frac{\partial m}{\partial x} = 0 \qquad 19c$$

along the bottom. Equation 19c is equivalent to the difference equation

$$m^2 \frac{W_o - W_u}{\Delta z} + m \frac{W_R - W_L}{\Delta x} - 2 W_o \frac{\partial m}{\partial x} = 0 \qquad 19d$$

A third method was devised to treat numerically the problem of the Gulf of California.

Let W and U be expanded in a Fourrier series:

$$W(xz) = \sum_{i=1}^{n} C_i(z) \cdot \sin(k_i x) \qquad 20a$$

$$U(xz) = \sum_{i=1}^{n} D_i(z) \cdot \cos(k_i x), \qquad 20b$$

where $$k_i = \frac{i\pi}{2L} \qquad 20c$$

These substitutions change the partial differential equation 15 into n total differential

equations

$$\frac{d^2 C_{i(z)}}{dz^2} + \frac{g \varphi_{(z)} k_i^2}{\sigma^2} C_{i(z)} = 0 \qquad 21a$$

Boundary condition 18a is already satisfied by 20a.

Boundary condition 18b gives

$$C_{i(0)} = 0 \qquad 21b$$

Substituting 20a and 20b into 18d we obtain

$$\sum_{i=1}^{n} C_{i(z)} \cdot \sin(k_i x) = m_{(x)} \sum_{i=1}^{n} D_{i(z)} \cdot \cos(k_i x)$$

Substituting 20a and 20b into 1c we obtain

$$-k_i D_{i(z)} = \dot{C}_{i(z)} \quad (\dot{C} \text{ denotes } \frac{dC}{dz})$$

Eliminating D between the last two equations, we obtain

$$\sum_{i=1}^{n} C_{i(z)} \cdot \sin(k_i x) + m_{(x)} \sum_{i=1}^{n} \frac{1}{k_i} \frac{dC_{i(z)}}{dz} \cos(k_i x) = 0 \qquad 21c$$

along the bottom. Let us define $W_{i(z)}$ (not the vertical velocity $W_{(xz)}$) by $C_{i(z)} = W_{i(z)} \cdot \dot{C}_{i(o)}$ 22a

Then $\dot{C}_{i(z)} = \dot{W}_{i(z)} \cdot \dot{C}_{i(o)}$ 22b

It follows directly from 22b that

$$\dot{W}_{i(o)} = 1 \qquad 22c$$

Substituting 22a,b, into 21a,b,c, we obtain the differential equations

$$\frac{d^2 W_{i(z)}}{dz^2} + \frac{g \varphi_{(z)} k_i^2}{\sigma^2} W_{i(z)} = 0 \qquad 23a$$

subject to the boundary conditions

$$W_i(o) = 0 \qquad 23b$$

and

$$W_i(z)\cdot\sin(k_i x) + \frac{dW}{dz}\frac{m(x)\cos(k_i x)}{k_i}\dot{C}_i(o) = 0 \qquad 23c$$

along the bottom.

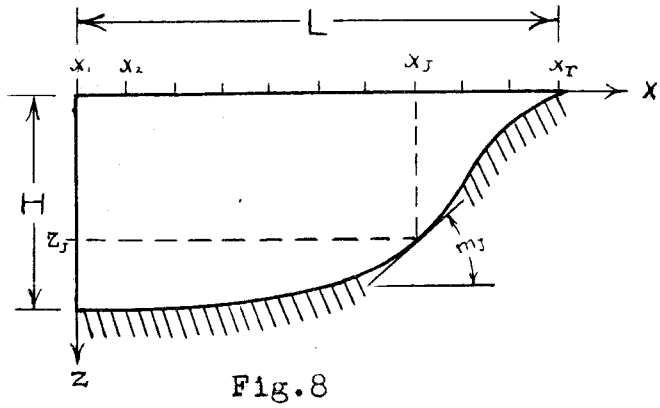

Fig.8

We have shown (page 23) that in the Fourier summations 20a and 20b "n" must be at least equal to two in order to provide consistency with all boundary conditions. It must be larger than two to give a satisfactory approximation. By making "n" sufficiently large we can approximate as closely as we wish any given velocity distribution.

A Fourier substitution yields therefore "n" differential equations of the type which Fjeldstad has developed for the case with constant depth. Each of these equations has its characteristic wave length λ, and indeed

$$\lambda_i = \frac{4L}{i} \qquad 23d$$

The internal wave can then be considered as the result of "n" internal waves of equal period but different wave length, superimposed upon one another. Each of these waves by itself satisfies boundary conditions at surface, but only all taken together can be made to satisfy the boundary condition at the bottom.

Let us then assume a definite value for the parameter σ. Each of the "n" equations 23a can be numerically integrated according to the method used by Fjeldstad for all values of "z" from 0 to H. Starting with 22c and 23b at the surface, we obtain values for $W_{i(z)}$ and $\dot{W}_{i(z)}$ at all depths.

Boundary condition 23c must now be applied. For that purpose divide the length L of the Gulf into r equidistant intervals with values of x ranging from $x_1 = 0$ to $x_r = L$. (Fig.8) Draw an accurate topographic section of the water body and find for all values of x_j ($j = 1,2,3,....r$) the corresponding slope m_j and depth z_j. Values for $W_{i(z_j)}$ and $\dot{W}_{i(z_j)}$ from the numerical integration are then obtained and K_{ji} numerically evaluated, where

$$K_{ji} = W_{i(z_j)} \cdot \sin(k_i x_j) + \dot{W}_{i(z_j)} \frac{m(x_j) \cdot \cos(k_i x_j)}{k_i} \qquad 24a$$

Boundary condition 23c becomes then simply

$$\sum_{j=1}^{r}\sum_{i=1}^{n} K_{ji}\dot{C}_{i(o)} = 0 \qquad 24b$$

This can be expanded into

$$K_{11}\dot{C}_{1(0)} + K_{12}\dot{C}_{2(0)} + \cdots\cdots K_{1i}\dot{C}_{i(0)} + \cdots\cdots K_{1n}\dot{C}_{n(0)} = 0 \qquad 25a$$

$$K_{21}\dot{C}_{1(0)} + K_{22}\dot{C}_{2(0)} + \cdots\cdots K_{2i}\dot{C}_{i(0)} + \cdots\cdots K_{2n}\dot{C}_{n(0)} = 0 \qquad 25b$$

$$\cdots\cdots\cdots\cdots\cdots\cdots\cdots\cdots\cdots\cdots\cdots\cdots\cdots\cdots$$

$$\cdots\cdots\cdots\cdots\cdots\cdots\cdots\cdots\cdots\cdots\cdots\cdots\cdots\cdots$$

$$K_{j1}\dot{C}_{1(0)} + K_{j2}\dot{C}_{2(0)} + \cdots\cdots K_{ji}\dot{C}_{i(0)} + \cdots\cdots K_{jn}\dot{C}_{n(0)} = 0 \qquad 25j$$

$$\cdots\cdots\cdots\cdots\cdots\cdots\cdots\cdots\cdots\cdots\cdots\cdots\cdots\cdots$$

$$\cdots\cdots\cdots\cdots\cdots\cdots\cdots\cdots\cdots\cdots\cdots\cdots\cdots\cdots$$

$$K_{r1}\dot{C}_{1(0)} + K_{r2}\dot{C}_{2(0)} + \cdots\cdots K_{ri}\dot{C}_{(0)} + \cdots\cdots K_{rn}\dot{C}_{n(0)} = 0 \qquad 25r$$

Hence we have one equation for each of the r points at the bottom boundary, and each equation contains n terms, referring to the n compoonents of the internal wave. In practice we shall choose r to be large compared to n.

If our parameter has been chosen corresponding to a true Eigenvalue of the differential equation, or in other words corresponding to a natural frequency of vibration of the Gulf, the boundary condition must be satisfied at all r points, and the r equations in n unknowns must be consistent.

In order to test consistence of equations 25, multiply

25a by K_{11}, ... 25j by K_{j1}, etc, and add to obtain 26a,

25a by K_{12}, ... 25j by K_{j2}, etc, and add to obtain 26b,

.....

.....

25a by K_{1i}, ... 25j by K_{ji}, etc, and add to obtain 26i etc.

In this manner we obtain "n" equations:

$$\left(\sum_{j=1}^{r} K_{j1}\cdot K_{j1}\right)\dot{C}_1(o) + \cdots \left(\sum_{j=1}^{r} K_{j1}\cdot K_{ji}\right)\dot{C}_i(o) + \cdots \left(\sum_{j=1}^{r} K_{j1}\cdot K_{jn}\right)\dot{C}_n(o) = 0 \quad (26a$$

$$\left(\sum_{j=1}^{r} K_{j2}\cdot K_{j1}\right)\dot{C}_1(o) + \cdots \left(\sum_{j=1}^{r} K_{j2}\cdot K_{ji}\right)\dot{C}_i(o) + \cdots \left(\sum_{j=1}^{r} K_{j2}\cdot K_{jn}\right)\dot{C}_n(o) = 0 \quad (26b$$

.....

.....

$$\left(\sum_{j=1}^{r} K_{ji}\cdot K_{j1}\right)\dot{C}_1(o) + \cdots \left(\sum_{j=1}^{r} K_{ji}\cdot K_{ji}\right)\dot{C}_i(o) + \cdots \left(\sum_{j=1}^{r} K_{ji}\cdot K_{jn}\right)\dot{C}_n(o) = 0 \quad (26i$$

.....

.....

$$\left(\sum_{j=1}^{r} K_{jn}\cdot K_{j1}\right)\dot{C}_1(o) + \cdots \left(\sum_{j=1}^{r} K_{jn}\cdot K_{ji}\right)\dot{C}_i(o) + \cdots \left(\sum_{j=1}^{r} K_{jn}\cdot K_{jn}\right)\dot{C}_n(o) = 0 \quad (26n$$

If they are consistent the determinant "D" will vanish:

$$D = \begin{vmatrix} \sum_{j=1}^{r} K_{j1}\cdot K_{j1} & \sum_{j=1}^{r} K_{j1}\cdot K_{j2} & \cdots & \sum_{j=1}^{r} K_{j1}\cdot K_{ji} & \cdots & \sum_{j=1}^{r} K_{j1}\cdot K_{jn} \\ \sum_{j=1}^{r} K_{j2}\cdot K_{j1} & \sum_{j=1}^{r} K_{j2}\cdot K_{j2} & \cdots & \sum_{j=1}^{r} K_{j2}\cdot K_{ji} & \cdots & \sum_{j=1}^{r} K_{j2}\cdot K_{jn} \\ \cdot & \cdot & \cdots & \cdot & \cdots & \cdot \\ \sum_{j=1}^{r} K_{ji}\cdot K_{j1} & \sum_{j=1}^{r} K_{ji}\cdot K_{j2} & \cdots & \sum_{j=1}^{r} K_{ji}\cdot K_{ji} & \cdots & \sum_{j=1}^{r} K_{ji}\cdot K_{jn} \\ \cdot & \cdot & \cdots & \cdot & \cdots & \cdot \\ \sum_{j=1}^{r} K_{jn}\cdot K_{j1} & \sum_{j=1}^{r} K_{jn}\cdot K_{j2} & \cdots & \sum_{j=1}^{r} K_{jn}\cdot K_{ji} & \cdots & \sum_{j=1}^{r} K_{jn}\cdot K_{jn} \end{vmatrix} \quad 27$$

In practice, since we have to choose "n" finite, this determinant will not vanish. However we may expect that for a proper choice of σ it will be a minimum.

For a first aproximation let "n" equal a

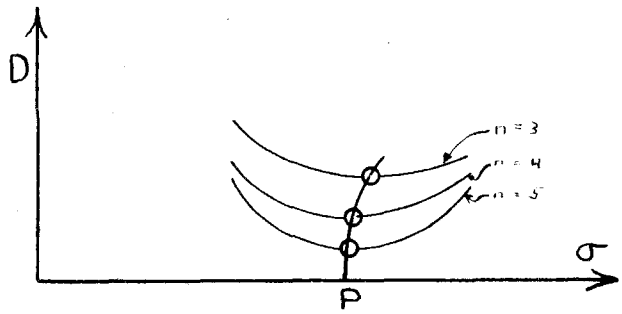

Fig. 9

small number, say three, and plot "D" against σ. (Fig.9) Then plot a similar curve for "n" equal to four, etc. Connect the minima of these curves and interpolate to D = 0. Point "P" represents the final value of our parameter σ.

The consistency of equations 25 may be tested by another method. Rewrite 25 for the case n = 3.

$$K_{j1}\dot{C}_{1(o)} + K_{j2}\dot{C}_{2(o)} + K_{j3}\dot{C}_{3(o)} = M_j \quad (j = 1,2,\ldots r) \qquad 28a$$

Let

$$\dot{C}_{2(o)} = X.\dot{C}_{1(o)} \qquad 28b$$

$$\dot{C}_{3(o)} = Y.\dot{C}_{1(o)} \qquad 28c$$

$$M_j = T_j.\dot{C}_{1(o)} \qquad 28d$$

We obtain

$$K_{j1} + K_{j2}.X + K_{j3}.Y = T_j \quad (j = 1,2,\ldots r) \qquad 29a$$

If equations 28a are exactly consistent, $M_j = 0$ and hence $T_j = 0$. This will not be the case in an actual investigation for finite values of "n". It appears reasonable to assume that if the parameter σ is properly chosen

$$\sum_{j=1}^{r} (T_j)^2 = \text{Minimum} \qquad 29b$$

or

$$\sum_{j=1}^{r} (K_{j1} + K_{j2}.X + K_{j3}.Y)^2 = \text{Minimum} \qquad 29c$$

Minimizing first with respect to X and Y,

$$\sum_{j=1}^{r} 2K_{j2}(K_{j1} + K_{j2}.X + K_{j3}.Y) = 0 \qquad 30a$$

$$\sum_{j=1}^{r} 2K_{j3}(K_{j1} + K_{j2}.X + K_{j3}.Y) = 0 \qquad 30b$$

Therefore

$$X = -\frac{\begin{vmatrix} \sum_{j=1}^{r} K_{j1}K_{j2} & \sum_{j=1}^{r} K_{j2}K_{j3} \\ \sum_{j=1}^{r} K_{j1}K_{j3} & \sum_{j=1}^{r} (K_{j3})^2 \end{vmatrix}}{\begin{vmatrix} \sum_{j=1}^{r} (K_{j2})^2 & \sum_{j=1}^{r} K_{j2}K_{j3} \\ \sum_{j=1}^{r} K_{j2}K_{j3} & \sum_{j=1}^{r} (K_{j3})^2 \end{vmatrix}} \qquad 31a$$

$$Y = -\frac{\begin{vmatrix} \sum_{j=1}^{r} (K_{j2})^2 & \sum_{j=1}^{r} K_{j1}K_{j2} \\ \sum_{j=1}^{r} K_{j2}K_{j3} & \sum_{j=1}^{r} K_{j1}K_{j3} \end{vmatrix}}{\begin{vmatrix} \sum_{j=1}^{r} (K_{j2})^2 & \sum_{j=1}^{r} K_{j2}K_{j3} \\ \sum_{j=1}^{r} K_{j2}K_{j3} & \sum_{j=1}^{r} (K_{j3})^2 \end{vmatrix}} \qquad 31b$$

From equations 31 we obtain the "relative weights" of the three components of the internal wave. Substituting their numerical value into the general expression for the vertical velocity component, (obtained from 20a, 22a, 28b, 28c):

$$W_{(xz)} = \left[W_{1(z)} \cdot \sin(k_1 x) + X \cdot W_{2(z)} \cdot \sin(k_2 x) + Y \cdot W_{3(z)} \cdot \sin(k_3 x)\right] \cdot \dot{C}_{1(o)} \qquad (32$$

we can find the distribution of the vertical velocity component throughout the entire channel.

Equation 29c can be rewritten

$$\sum_{j=1}^{n} K_{j1}(K_{j1} + K_{j2} \cdot X + K_{j3} \cdot Y) + \sum_{j=1}^{n} (K_{j2} + K_{j3}) \cdot (K_{j1} + K_{j2} \cdot X + K_{j3} \cdot Y) = \text{Minimum}$$

The last term vanishes as result of 30, and we have simply

$$\sum_{j=1}^{n} (K_{j1})^2 + X \cdot \sum_{j=1}^{n} K_{j1} \cdot K_{j2} + Y \cdot \sum_{j=1}^{n} K_{j1} \cdot K_{j3} = \text{Minimum} \qquad 33$$

The procedure is now similar to that of page 36. Denote the minimum of equation 33 by "M", and evaluate "M" for several values of σ. Plot $M = f(\sigma)$ for various values of "n", analogous to the curves $D = f(\sigma)$ in figure 9, and interpolate to obtain final value of parameter. The various terms of which "M" is composed are very similar to those of "D", and only little additional work is necessary to obtain values for "M".

The general procedure followed in finding a solution for the differential equation 15 was first to assume a definite value for the parameter. Considering the boundary conditions at the surface and the open end of the channel the distribution of vertical velocity was then computated. If the parameter has been properly chosen, values from this computation near the bottom will satisfy the bottom boundary condition. The parameter then corresponds to a period of free vibration of the water mass. The author believes that this procedure, complicated as it may seem, nevertheless represents the most accurate and the fastest possible method.

Internal Waves
in Case of a Horizontal Density Gradient

The velocity of propagation of an internal wave depends upon depth and density distribution. In our previous discussion, referring to the Gulf of California, it was possible to consider the equilibrium density ρ_o a function of depth only. In river-fed channels with low densities at the river mouth, in large oceans where density changes with latitude, a variation of along the horizontal coordinate may become appreciable.

We shall use the same notation as in the previous development but note that ρ_o, p_o, k, and c are functions of coordinate x. Graphs of density anamolies against depth will differ for different points in a channel; nevertheless the actual horizontal gradient remains extremely small, and almost always

$$\frac{\partial p_o}{\partial x} \ll \frac{\partial p_1}{\partial x}$$

We arrive again at equation 4. Since we shall deal here with a basin of constant depth only, the following solutions have proven to be consistent:

$$w(xzt) = W(z)\sin(kx)\cos(\sigma t) \qquad 5a$$

$$u(xzt) = U(z)\cos(kx)\cos(\sigma t) \qquad 5b$$

$$p_1(xzt) = P_1(z)\sin(kx)\sin(\sigma t) \qquad 5c$$

$$\rho_1(xzt) = R_1(z)\sin(kx)\sin(\sigma t) \qquad 5d$$

where "k" is a function of "x".

$$\text{Let } \lambda_{(x)} = \left(1 - \frac{x}{c} \cdot \frac{dc}{dx}\right) \cdot \frac{1}{c} \qquad 34a$$

$$\text{Then } \frac{\partial(kx)}{\partial x} = k + x\frac{dk}{dx}$$

$$\frac{\partial(kx)}{\partial x} = \frac{\sigma}{c}\left(1 - \frac{x}{c}\frac{dc}{dx}\right)$$

$$\frac{\partial(kx)}{\partial x} = \sigma\lambda \qquad 34b$$

Substituting equations 5 into 4, we can eliminate all trigonometric terms:

$$-\sigma U + \frac{P_1}{\rho_0}\sigma\lambda = 0 \qquad 35a$$

$$-\sigma W + \frac{g R_1}{\rho_0} + \frac{1}{\rho_0}\frac{\partial P_1}{\partial z} = 0 \qquad 35b$$

$$-\sigma\lambda U + \frac{\partial W}{\partial z} = 0 \qquad 35c$$

$$\sigma R_1 + \frac{\partial \rho_0}{\partial z} W = 0 \qquad 35d$$

Eliminating U from 35a and 35c and differentiating:

$$\frac{\partial P_1}{\partial z} = \frac{1}{\sigma\lambda^2}\left[\frac{dW}{dz}\frac{\partial \rho_0}{\partial z} + \rho_0 \frac{d^2W}{dz^2}\right] \qquad 36$$

Substituting 36 and 35d into 35b we obtain the desired differential equation in W:

$$\frac{d^2W}{dz^2} + \frac{dW}{dz}\left[\frac{1}{\rho_0}\frac{\partial \rho_0}{\partial z}\right] + W\left[-\sigma^2\lambda^2 - \frac{g\lambda^2}{\rho_0}\frac{\partial \rho_0}{\partial z}\right] = 0 \qquad 37$$

In view of 14b and 14c we obtain finally

$$\frac{d^2W}{dz^2} + \lambda^2 g \varphi W = 0 \qquad 38$$

It can be shown that a substitution of the form 16 will lead to the identical result.

This equation is identical in form with that derived for constant density distribution (6a), but in that case

$$\lambda = \frac{1}{c} \qquad 6a$$

while here $\lambda = \frac{1}{c}\left[1 - \frac{x}{c}\frac{dc}{dx}\right]$ 34a

which reduces to the above case if c remains constant.

Rewrite equation 34a

$$\frac{dc}{dx} = \left(\frac{1}{x}\right)c + \left(-\frac{\lambda}{x}\right)c^2$$

and let $c = \frac{1}{v}$

The equation is then reduced to linear form

$$\frac{dv}{dx} + \left(\frac{1}{x}\right)v = \frac{\lambda}{x}$$

with the solution

$$v = \frac{1}{x}\left[K + \int_0^x \lambda\, dx\right.$$

or

$$c = \frac{x}{\int_0^x \lambda\, dx} \qquad 39$$

K = 0 since c does not vanish for x = 0.

This method has been carried out for a basin of constant depth, but can also be used for a sloping bottom, if this slope is sufficiently small.

Let "H" represent the depth of maximum vertical velocity,

"h" represent the depth to the bottom.

From a numerical integration, analogous to that of Fjeldstad (page 50) we obtain values for W and $\frac{dW}{dz}$ throughout the entire depth.

W_H represents the maximum vertical velocity.

$$W_h = m.U_h = \frac{m}{\sigma\lambda}\left(\frac{dW}{dz}\right)_h \quad (35c).$$

If $W_h \ll W_H$

or $$m \ll \frac{\sigma W_H}{c\left(\frac{dW}{dz}\right)_h} \qquad 40$$

Fjeldstad's numerical integration method may be employed, since W_h may then be assumed equal to zero for all practical purposes.

We may wish to calculate periods of free vibration of various water bodies. Note that $c.dt = dx$, and hence the time necessary for a wave to cover the entire length of a channel of length "L" is

$$t = \int_0^L \frac{1}{c}\, dx \qquad 41a$$

In case of a half open channel $t = 1/4\ T_1$, $t = 3/4\ T_2$, $t = 5/4\ T_3$, etc, referring to waves of first, second and third harmonic. We obtain generally

$$T_i = \frac{4}{2i - 1} \int_0^L \frac{1}{c}\, dx \qquad 41b$$

A Method of Numerical Solution

1: Draw a xz cross-section with a sufficient number of isopycnal lines (referring to a density distribution in the undisturbed state) to permit the calculation of φ.

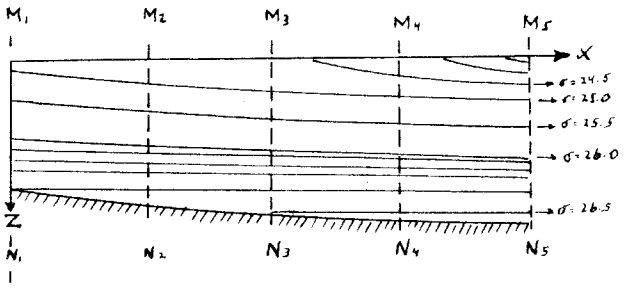

2: For various sections M-N plot φ against depth. Values of φ are obtained from above graph.

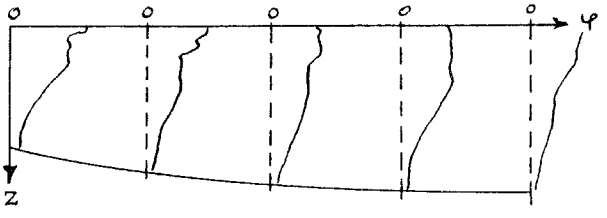

3: For each section M-N Fjeldstad's method of numerical integration (page 50) should be applied, using values as obtained in (2), and if condition 40 is fullfilled, taking into consideration the change of depth.

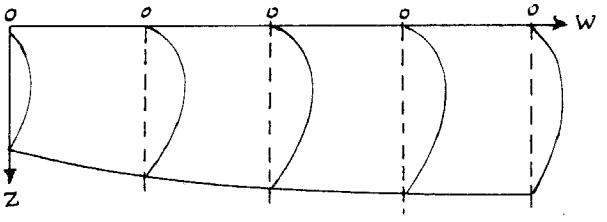

4: For each of these sections corresponding to different values of x a paramter will be obtained from above integration. Plot $\lambda = f(x)$, and $\int_0^x \lambda\,dx = f(x)$

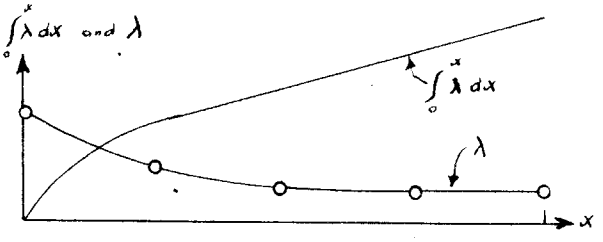

5: Referring to equation 39 we now plot velocity of propagation

$c = f(x)$

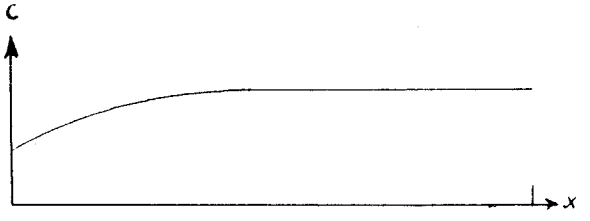

6: Plot $\frac{1}{c} = f(x)$ and

integrate over the entire length L of the channel. This integral, substituted into 41b will give the periods of free vibration.

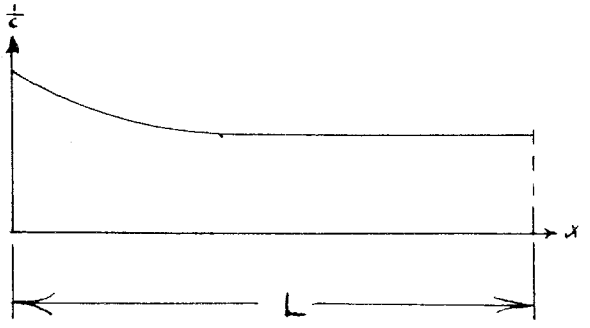

Fig.10

Numerical Results

Fjeldstad's theory for basins of constant depth was applied to the outer portion of the Gulf of California. (Equation 6a, and pages 50, 51, 52) Figure 13 illustrates the results obtained by this theory. They compare favorably with those obtained from observation:

	c	H
Theory	167 cm/sec	500m - 600 m
Observation	175 cm/sec	675 m.

where c represents the velocity of propagation, H the depth of maximum amplitude of oscillation.

The period of oscillation "T" was calculated by considering the Gulf a basin of variable depth, the density of the water constant with respect to the horizontal coordinate, and employing the theory developed in this paper. The investigation was carried out for three values of "i" only, i = 4,5,and 7, hence the internal wave in the Gulf was considered a super-position of three internal waves of constant wave-length.

The following table illustrates why values of i = 4, i = 5, i = 7, corresponding to wave-lengths of 1000km, 800km, 570 km were chosen. (Equation 23d)

Values of i	5-6-7	3-4-5-	4-5-6	4-5-7
$D \times 10^{-27}$ (Equ. 27)	130.067	123.337	63.185	25.017

T = 6.4 days

A sample calculation (pages 53-56) illustrates the method followed in obtaining the following results:

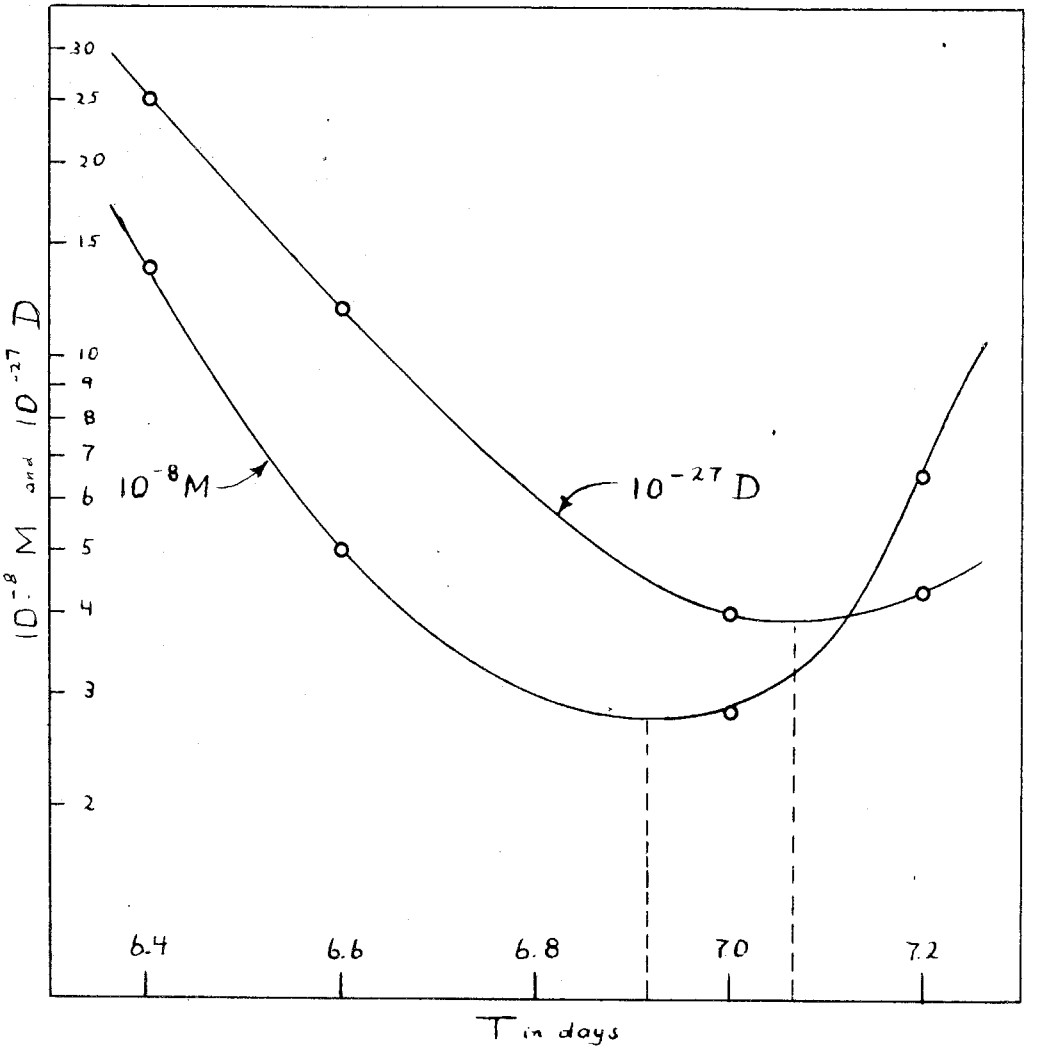

Fig.11

T in days	6.4	6.6	7.0	7.2
D x 10^{-27} (Equ. 27)	25.017	11.753	3.915	4.229
X (Equ. 31a)	0.459	0.139	-0.1163	-0.242
Y (Equ. 31b)	0.239	-0.085	-0.313	-0.105
M x 10^{-8} (Equ. 33)	13.85	4.94	2.82	6.57

$i_1 = 4$
$i_2 = 5$
$i_3 = 7$

A semi-logarithmic scale in figure 11 helps to emphasize the location of the minima.

A fair agreement between theory and observation can be shown:

T from curve D = f(T): 7.07 days

T from curve M = f(T): 6.92 days

T from observation ..: 6.6 days

Conclusion

Figure 13 indicates a maximum horizontal velocity of 20 cm/sec at the bottom of the Gulf. This velocity is large enough to exert a pronounced influence upon sedimentation. If we consider a standing wave the horizontal velocity component will reach a maximum near the location of nodes, and we might expect that only large-sized particles could settle in their vicinity. On the other hand anti-nodes are characterized by very small horizontal currents, which would permit small particles to be deposited at the bottom.

Dr. Revelle has measured the sizes of particles from various bottom samples, and they indicate the existance of three nodes. Only few measurements are available and the evidence is not conclusive, but it suggests strongly that the particular wave-form of fourth order with respect to the horizontal axis (page 15) does not constitute an isolated phenomenon but appears to be of common occurence.

Such a wave might be caused by an outside periodic disturbance, the period of the disturbance being closely related to that of the Gulf. The lunar-fortnightly tide has a period of 13.6 days, (2 x 6.8 days) but its strength is only one sixth

the strength of the principle lunar tide. Weather maps do not indicate a periodic disturbance in the Gulf region.

The cause for the predominance of a particular overtone may lie in the topography of the region. Only a rectangular basin is equally suitable to all overtones, a non-linear topography might favor only a very limited number of overtones. In that case a single atmospheric disturbance would suffice to set up oscillations of this frequency, which would prevail for a great length of time since the damping factor is small. An investigation of our curves for other frequencies should fail to procure minima as pronounced as those in figure 11.

Another expedition into the Gulf of California has been planned for the fall of 1940. Measurements relating to internal waves will again be taken. They should prove especially interesting in the light of this investigation.

SAMPLE CALCULATION

Fjeldstad's Method of Numerical Integration for Constant Depth

1. Obtain φ (14b) as function of depth from direct measurements of density. See Figure 12.
2. Assume $W_0 = 0$, $\dot{W}_0 = 1$.
3. $$W_{10} = W_0\left(1 - \lambda^2 g(\Delta z)^2 \frac{2\varphi_0 - \varphi_1}{6}\right) + \dot{W}_0(\Delta z)\left(1 - \lambda^2 g(\Delta z)^2 \frac{5\varphi_0 - 3\varphi_1}{48}\right)$$
   $(\Delta z = 1000)$ *

   Using $z = 2000$, $z = 3000$, calculate W_{20}, W_{30}
4. $\Delta_1 W_0 = W_{10} - W_0 \qquad \Delta_1 W_{10} = W_{20} - W_{10}$
5. $\Delta_2 W_0 = \Delta_1 W_{10} - \Delta_1 W_0$
6. $V_n = -\lambda^2 g \varphi_0 (\Delta z)^2 . W_n$ From this general formula obtain V_0, V_{10}, V_{20}.
7. $\Delta_1 V_n = V_{n-1} - V_n$ From this find $\Delta_1 V_0$ and $\Delta_1 V_{10}$
8. $\Delta_2 V_n = \Delta_1 V_{n-1} - \Delta_1 V_n$ From this obtain $\Delta_2 V_0$
9. $\Delta_2 W_n = V_{n-1} + \frac{1}{12}\Delta_2 V_{n-1}$ From this obtain $\Delta_2 W_{10}$
10. $\Delta_1 W_n = \Delta_1 W_{n-1} + \Delta_2 W_{n-1}$ From this obtain $\Delta_1 W_{20}$
11. $W_n = W_{n-1} + \Delta_1 W_{n-1}$ From this obtain W_{30}

    Find V_{30} from (6), etc.
12. Interpolation: $W_{n-\frac{1}{2}} = W_n - \frac{\Delta_1 W_n + \Delta_1 W_{n-1}}{4} + \frac{\Delta_2 W_n}{5}$

Results from integration in figure 13.

* All equation are given for cgs units.

Sample Calculation

$\lambda^2 g = 3.62 \times 10^{-2}$ c = 167 cm/sec

1	2	3	4	5	6	7	8
Depth in m.	$10^8 \varphi$	$10^{-4} W$	$\Delta_1 W$	$\Delta_2 W$	V	$\Delta_1 V$	$\Delta_2 V$
0	2.20	0.0000			0.0		
			1000			-2.0	
10	5.52	0.1000		-2	-2.0		-1.6
			998			-3.6	
20	7.74	0.1998		-6	-5.6		2.3
			992			-1.3	
30	6.40	0.2990		-7	-6.9		1.5
			985			0.2	
40	4.68	0.3975		-7	-6.7		-4.6
			978			-4.4	
50	6.20	0.4953		-11	-11.1		-6.5
			967			-10.9	
60	10.32	0.5920		-23	-22.0		6.1
			944			-4.8	
70	10.80	0.6864		-26	-26.8		4.6
			918			-0.2	
80	9.60	0.7782		-27	-27.0		-0.9
			891			-1.1	
90	8.96	0.8673		-28	-28.1		
			863				
100	8.28	0.9536					
			9536	-137			
60	10.32	0.5920			-88		
			1862			-20	
80	9.60	0.7782		-108	-108		14
			1754			-6	
100	8.28	0.9536		-113	-114		33
			1641			27	
120	5.36	1.1177		-84	-87		-9
			1557			18	
140	3.76	1.2734		-70	-69		-6
			1487			12	
160	2.80	1.4221		-57	-57		-8
			1430			4	
180	2.36	1.5651		-54	-53		-1
			1376			3	
200	2.04	1.7027		-50	-50		-2
			1326			1	
220	1.84	1.8353		-49	-49		0
			1277			1	
240	1.71	1.9630		-48	-48		-2
			1229			-1	
260	1.63	2.0859		-49	-49		-1
			1180			-2	
280	1.60	2.2039		-51	-51		
			1129				
300	1.59	2.3168	17248	-773			

1	2	3	4	5	6	7	8
200	2.04	1.7027			-314		
			3239			8	
250	1.67	2.0266		-337	-306		-36
			2902			-28	
300	1.59	2.3168		-337	-334		-29
			2565			-57	
350	1.68	2.5733		-393	-391		60
			2172			3	
400	1.54	2.7905		-383	-388		-1
			1789			2	
450	1.44	2.9694		-386	-386		-4
			1403			-2	
500	1.38	3.1097		-388	-388		5
			1015			3	
550	1.32	3.2112		-385	-385		42
			630			45	
600	1.15	3.2742		-337	-340		10
			293			55	
650	0.99	3.3035		-294	-295		
			-1				
700	0.80	3.3034					
			16007	-3240			
500	1.38	3.1097			-1550		
			1645			190	
600	1.15	3.2742		-1353	-1360		211
			292			401	
700	0.80	3.3034		-940	-959		-262
			-648			139	
800	0.70	3.2386		-844	-820		-56
			-1492			83	
900	0.66	3.0894		-742	-737		84
			-2234			167	
1000	0.55	2.8660		-563	-570		-19
			-2797			148	
1100	0.45	2.5863		-424	-422		-61
			-3221			87	
1200	0.41	2.2642		-340	-335		-7
			-3561			80	
1300	0.37	1.9081		-256	-255		-2
			-3817			78	
1400	0.32	1.5264		-177	-177		-15
			-3994			63	
1500	0.28	1.1270		-115	-114		-14
			-4109			49	
1600	0.25	0.7161		-66	-65		-9
			-4175			40	
1700	0.23	0.2986		-26	-25		
			-4201				
1800	0.21	-0.1215					
			-32312	-5846			

SAMPLE CALCULATION

of a Point in Figure 11.

L = 1000 km.

Columns 10 and 11.	Defined by equation 22a Corresponds to columns 3 and 4 of previous sample calculation.
Column 12.	Defined by equation 22b. Divide corresponding vlues in column 11 by z.
Columns 14,15,16.	Obtain from a topographic map (Figure 4)
Column 17, 18.	k_7 as defined by equation 20c
Column 19	Column 10 multiplied by corresponding values of column 17
Column 20	Column 12 multiplied by corresponding values of column 18
Column 21	Defined by equation 24a. Add Column 19 to column 20.
Column 22 and 23.	Obtained by the same procedure employed to calculate column 21, using values of i = 4, i = 5.
Columns 24 - 29.	By multiplication of column 21, 22, and 23.

By adding these products we obtain the sums,

necessary for the calculation of D, X, Y, M.

D as defined by equation 27 = 4.229×10^{27}

X as defined by equation 31a = -0.2420

Y as defined by equation 31b = -0.1053

M as defined by equation 33 = 6.57×10^{8}

Sample Calculation

T = 7.2 days

9	10	11	9	10	11
Depth in m.	$W_7(z) \cdot 10^{-4}$	$\Delta, W_7(z)$	Depth in m.	$W_7(z) \cdot 10^{-4}$	$\Delta, W_7(z)$
0	0.0000		450	0.6463	
		999			-2131
10	0.0999		500	0.4332	
		993			-2315
20	0.1992		550	0.2017	
		974			-2393
30	0.2966		600	-0.0376	
		953			-2380
40	0.3919		650	-0.2756	
		932			-2306
50	0.4851		700	-0.5062	------
		896	----------		-4192
60	0.5747		800	-0.9254	
		815			-3447
70	0.6562		900	-1.2701	
		736			-2471
80	0.7298		1000	-1.5172	
		639			-1515
90	0.7937		1100	-1.6687	
		557			-643
100	0.8494	----	1200	-1.7330	
----------		872			193
120	0.9366		1300	-1.7137	
		644			931
140	1.0010		1400	-1.6206	
		465			1533
160	1.0415		1500	-1.4673	
		326			2014
180	1.0801		1600	-1.2659	
		205			2387
200	1.1006		1700	-1.0272	
		109			2664
220	1.1115		1800	-0.7608	
		12	----------		
240	1.1127				
		-76			
260	1.1051				
		-160			
280	1.0891				
		-241			
300	1.0650	------			
----------		-913			
350	0.9737				
		-1399			
400	0.8338				
		-1875			

i = 7

$\frac{gk^2}{\sigma^2} = 1.17 \times 10^{-1}$

9	10	11	12
Depth in m.	$W_7(z) \cdot 10^{-4}$	$\Delta, W_7(z)$	$\dot{W}_7(z)$
250	1.1092	-76	-0.0380
900	-1.2701	-2959	-0.2959
1250	-1.7270	193	0.0193
1500	-1.4673	1773	0.1773
1655	-1.1361	2406	0.2406
1735	-0.9362	2622	0.2622
1775	-0.8260	2733	0.2733
1790	-0.7892	2826	0.2826
1798	-0.7665	2838	0.2838
1799	-0.7636	2842	0.2842
1800	-0.7608	2844	0.2844

13	14	15	16	17	18	19	20	21
j	x in km	z in m	slope x 10^5	$\sin(k_7 x)$	$\frac{m\cos(k_7 z)}{k_7}$	$W_{7(z)} \sin k_7 x \times 10^{-4}$	$\frac{\dot{W}_7(z) \cdot m\cos(k_7 x)}{k_7} \cdot 10^{-4}$	$K_{7j} \cdot 10^{-4}$
1	0	1800	0	.0000	0	0.0000	0	.0000
2	50	1800	0	.5225	0	-0.3975	0	-.3975
3	100	1800	0	.8910	0	-0.6779	0	-.6779
4	150	1800	0	.9969	0	-0.7584	0	-.7584
5	200	1800	0	.8090	0	-0.6155	0	-.6155
6	250	1800	0	.3827	0	-0.2912	0	-.2912
7	300	1800	0	-.1564	0	0.1190	0	.1190
8	350	1800	0	-.6495	0	0.4941	0	.4941
9	400	1800	0	-.9511	0	0.7236	0	.7236
10	450	1800	0	-.9724	0	0.7398	0	.7398
11	500	1800	0	-.7071	0	0.5380	0	.5380
12	550	1799	-1.7	-.2334	-150	0.1782	-.0043	.1739
13	600	1798	-7.5	.3090	-650	-0.2368	-.0184	-.2552
14	650	1790	-20	.7604	-1170	-0.6001	-.0331	-.6332
15	700	1775	-55	.9877	-782	-0.8158	-.0214	-.8372
16	750	1735	-100	.9240	3480	-0.8650	.0912	-.7738
17	800	1655	-250	.5878	18400	-0.6678	.4427	-.2251
18	850	1500	-400	.0785	36800	-0.1152	.6525	.5373
19	900	1250	-570	-.4540	46200	0.7841	.0892	.8733
20	950	900	-970	-.8526	46100	1.0829	-1.3641	-.2812
21	1000	250	-20	-1.0000	0	-1.1092	0	-1.1092

13	22	23	24	25	26	27	28	29
j	K_{4j}	K_{5j}	$K_{4j}K_{4j}$	$K_{4j}K_{5j}$	$K_{4j}K_{7j}$	$K_{5j}K_{5j}$	$K_{5j}K_{7j}$	$K_{7j}K_{7j}$
1	0.0000	0.0000	0.0000	0.0000	0.0000	0.0000	0.0000	0.0000
2	-0.1691	-1.1112	0.0286	0.1879	0.0672	1.2348	0.4417	0.1580
3	-0.3216	-2.0531	0.1034	0.6603	0.2180	4.2152	1.3918	0.4595
4	-0.4426	-2.6826	0.1959	1.1873	0.3357	7.1963	2.0345	0.5752
5	-0.5203	-2.9036	0.2707	1.5107	0.3203	8.4309	1.7872	0.3788
6	-0.5471	-2.6826	0.2993	1.4677	0.1593	7.1963	0.7812	0.0848
7	-0.5203	-2.0531	0.2707	1.0682	-0.0619	4.2152	-0.2443	0.0142
8	-0.4426	-1.1112	0.1959	0.4918	-0.2187	1.2348	-0.5490	0.2441
9	-0.3216	0.0000	0.1034	0.0000	-0.2327	0.0000	0.0000	0.5236
10	-0.1691	1.1112	0.0286	-0.1879	-0.1251	1.2348	0.8221	0.5473
11	0.0000	2.0531	0.0000	0.0000	0.0000	4.2152	1.1047	0.2894
12	0.1567	2.6775	0.0246	0.4196	0.0027	7.1690	0.4656	0.0302
13	0.2750	2.8980	0.0756	0.7970	-0.0702	8.3984	-0.7396	0.0651
14	0.3272	2.6864	0.1071	0.8790	-0.2072	7.2167	-1.7010	0.4009
15	0.3010	2.1375	0.0906	0.6434	-0.2520	4.5689	-1.7895	0.7009
16	0.2674	1.4142	0.0715	0.3782	-0.2069	2.0000	-1.0943	0.5988
17	0.4552	1.1900	0.2072	0.5417	-0.1025	1.4161	-0.2679	0.0507
18	0.9809	1.1834	0.9622	1.1608	0.5270	1.4004	0.6358	0.2887
19	1.7832	1.8573	3.1798	3.3119	1.5573	3.4496	1.6220	0.7627
20	2.3601	2.9515	5.5701	6.9658	-0.6637	8.7114	-0.8300	0.0791
21	-0.1891	1.7463	0.0358	-0.3302	0.2097	3.0496	-1.9370	1.2303
		Σ	11.8210	21.1532	1.2562	86.5536	1.9340	7.4823

All numbers to be multiplied by 10^4
in order to comform with theory (24a)

Density Anamolies

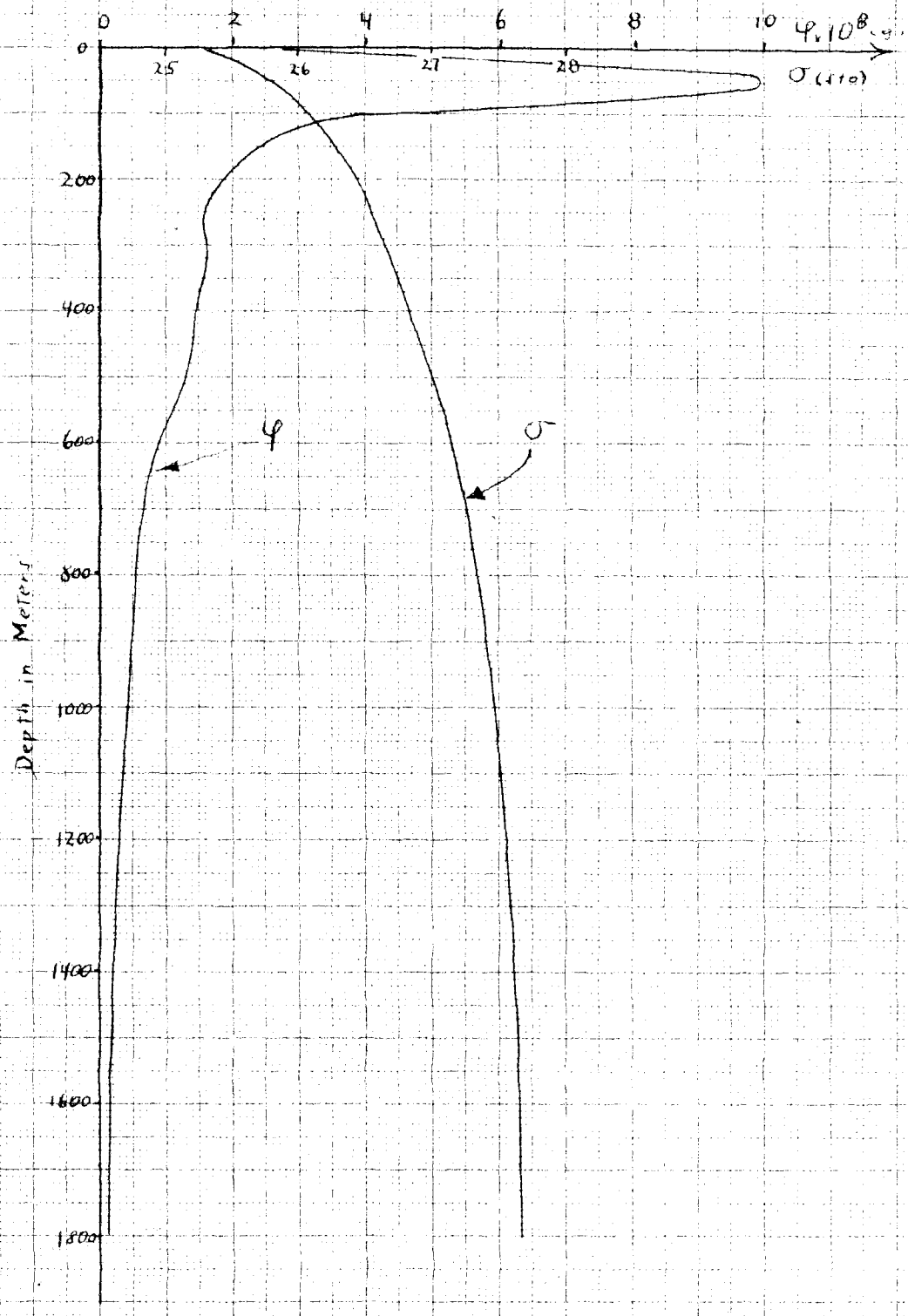

Figure 12

Distribution of Horizontal and Vertical Velocity Component and of vertical Displacement with Depth

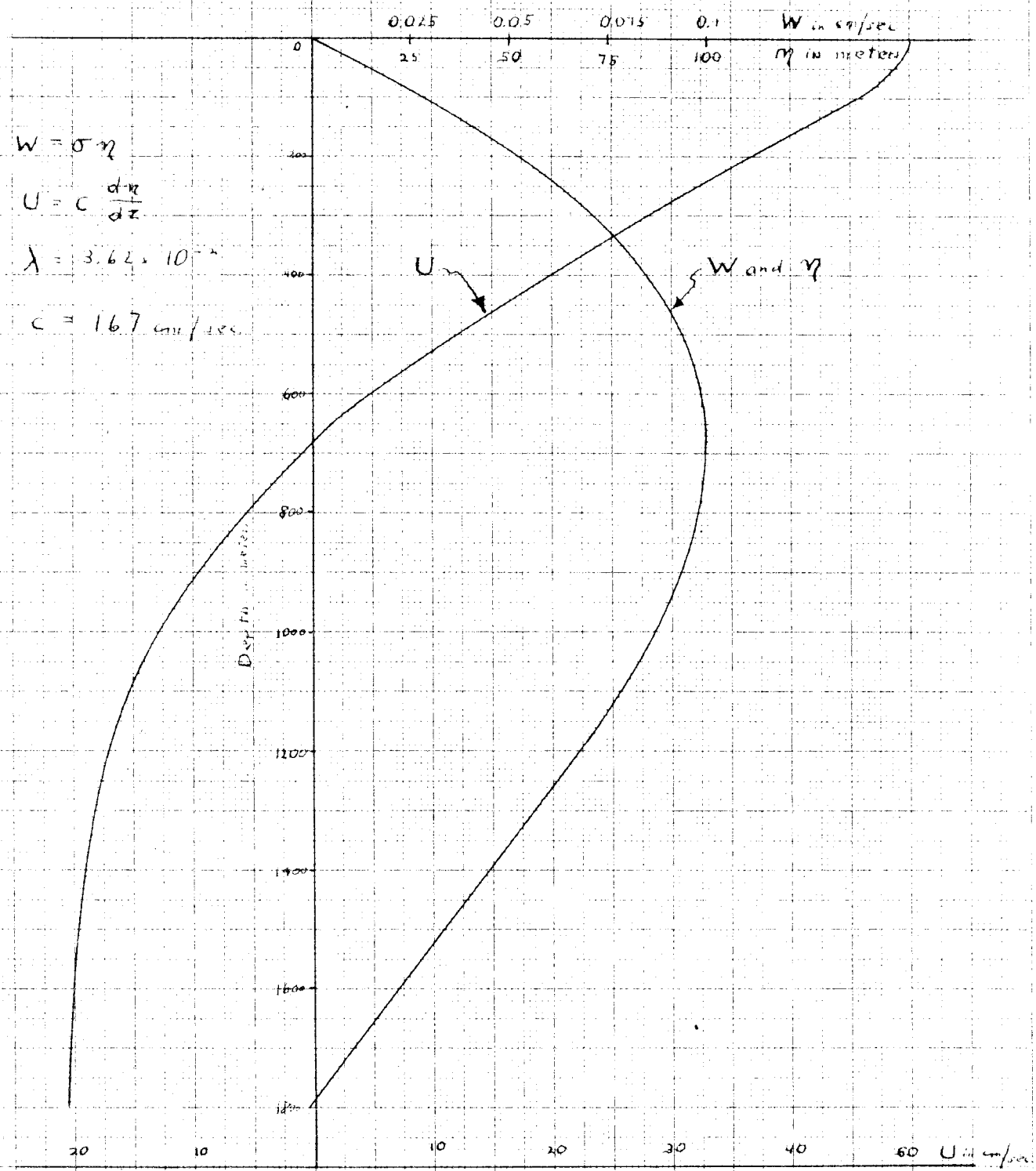

$W = \sigma \eta$

$U = C \frac{d\eta}{dz}$

$\lambda = 3.62 \times 10^{-4}$

$C = 167$ cm/sec.

Figure 13

References

1. FJELDSTAD, J.E. Interne Wellen. Geofysiske Publikasjoner. Vol. X. No. 6, 1933

2. DEFANT, A. Dynamische Ozeanographie. Einführung in die Geophysik III, 1929. p. 154-155, 176, 178, 187-190.

3. Lamb, H. Hydrodynamics. VI Edition, 1932. p. 370-372.

4. SVERDRUP, JOHNSON AND FLEMING: The Oceans, their Physics, Chemistry and general Biology.

5. Th. SEXL. Zeitschrift für Physik. Vol.87, p.105-126

6. Th. SEXL. Zeitschrift für Physik. Vol.99 p.751-775